Journal of Thermal Science Vol.29, No.5 (2020) 1300−1308

https://doi.org/10.1007/s11630-020-1292-4 **Article ID: 1003-2169(2020)05-1300-09**

A New Hybrid System Design for Thermal Energy Storage

CEYLAN İlhan[1], ALI Ismail Hamad Guma[1], ERGÜN Alper[1*], GÜREL Ali Etem[2], ACAR Bahadır[1], İSLAM Nursel[1]

1. Department of Energy Systems Engineering, Faculty of Technology, Karabük University, Karabük 78050, Turkey
2. Department of Mechanical and Manufacturing Engineering, Faculty of Technology, Duzce University, Düzce 81620, Turkey

Abstract: Due to some serious environmental problems like global warming and greenhouse effect, studies on solar energy systems are being conducted all over the world. The studies conducted in recent years are on hybrid designs in which solar energy systems can realize both electricity and heat production at the same time. In this way, both electrical energy and heat energy can be generated from the same system In this study, the design and analysis of a concentrated solar air collector with a heat storage unit were carried out. In the solar air collector, heat energy was depot in paraffin wax, and the electrical energy which was stored in the battery using the PV (photovoltaic) modules in the system enabled the operation of the system fan. The experiments which aimed at determining system performance were carried out in winter when the ambient temperature was low. The experiments were performed with or without a heat storage unit, and a comparative analysis was made. It was found that the temperature of the air released from the collector ranged from 15°C to 40°C when the exterior temperature was −5°C. The average efficiency of the concentrated system without the heat storage unit was calculated as 67%. The average efficiency of the concentrated system with the heat storage unit was calculated as 96%.

Keywords: heat storage, phase change material, concentrated solar air collector

1. Introduction

The interest in solar energy is increasing continually. Scientists are developing new technologies and methods to exploit this renewable resource. Solar energy has been used in many different applications over the years, one of the most important of which is heating applications with solar collectors. Solar radiation is transferred to fluid as heat energy with solar collectors. The most used fluid is water, since it has a high heat capacity. Today, air is also used in solar collectors. However, water is preferred as it transfers heat well. Although this situation prevents the widespread use of solar air collectors, the increasing need for energy has shown that solar air collectors can also be used in different areas efficiently [1–3]. When the studies on solar air collectors are examined, it is seen that Zheng et al. [4] developed a mathematical model by examining the performance of a new metal corrugated packed air collector in buildings in cold areas. The study revealed that the use of metal corrugated packed solar air collectors is appropriate in rural areas in cold regions due to their high heat transfer coefficient and economic performance. Abuşka and Şevik [5] performed V-groove air collectors with the 4E (energy, exergy, economic and

Received: Apr 11, 2019 AE: RENNO Carlo Corresponding author: ERGÜN Alper E-mail: alperergun@karabuk.edu.tr

Nomenclature

A_m	module area/m²	STC	standard test condition
AM	air mass	*T*	temperature/°C
AR	area ratio	*U*	uncertainties
a	sensitivity	UTC	unglazed solar air collector
a-Si	amorphous silicon	*V*	voltage
CdTe	cadmium telluride	*W*	Watt
CE	concentrator efficiency	X_i	observations conducted
CIS	copper indium selenium	X_m	arithmetic mean of observations
CR	concentrator rate	**Greek symbols**	
c	specific heat/kJ·kg^{-1}·K^{-1}	α	absorptivity
h	enthalpy/kJ·kg^{-1}	β	thermal coefficent
$I_{(t)}$	solar radiation/W·m^{-2}·K^{-1}	δ	packing factor
I	current/A	η	efficiency
L	latent heat	ρ	density/kg·m^{-3}
P	power/W	τ	transparency
PAP	performance absorber plate	**Subscripts**	
PCM	phase change material	c	cell
PV	photovoltaic	f	fan
PV/T	photovoltaic thermal	l	liquid
$\dot{Q}$	rate of thermal energy/kW	m	module
RMSE	root mean square error	s	solid
S	standard deviation	u	useful

environmental) analyses. V-groove air collectors were made of copper and aluminum plate. The researchers calculated that the average energy efficiency of solar air collectors was 43% to 60%, while their exergy efficiency was 6%–12%. They argued that despite their high cost, in particular V-groove solar air collectors must be preferred because of their performance. In their study, Gulcimen et al. [6] examined the drying of sweet basil with solar air collector and observed that the collector efficiency ranged between 23% and 69% depending on the changing air speed. Li et al. [7] used different absorbent surfaces to find a solution to the problem of low thermo-physical properties of air in air collectors, and they found that heat transfer coefficient, pressure drop, and performance increased as the absorbent surface area enlarged. El Khadraoui et al. [8] designed an indirect-type forced convection solar dryer using paraffin-wax as the phase change material (PCM). The tests they conducted under load with and without the PCM revealed that in the system with the PCM, the temperature of the drying chamber was found to be 4°C to 16°C higher than the ambient temperature all through the night, while the relative humidity was calculated as 17% to 34.5%.

In their study, Bahrehmand et al. [9] developed a mathematical model to simulate the thermal behavior of single and double-glazed solar air collectors under forced convection conditions. Hernandez and Quinonez [10] compared the measured and simulated values by experimentally validating an analytical model accounting for the thermal behavior of natural convection dual parallel flow solar air collectors. They found that the *RMSE* values were less than 6% for outlet air temperature and available energy obtained by the collector. Demou and Grigoriadis [11] calculated the yearly energy efficiency of the solar air collectors in a one-dimensional model, which they formed considering the regional meteorological specifications, the effects of the geometric design, and the materials used. In their study, Al-damook and Khalil [12] experimentally and theoretically investigated the benefits of using a perforated absorbent plate (PAP) and an unglazed solar air collector (UTC) under the climatic conditions of West Iraq. Comparing the thermal performance and economic characteristics of the collector with other heating systems, they found that such collectors offer economic and thermal benefits in western Iraq climatic condition in winter season. Al-Sulaiman et al. [13] conducted the performance analysis of a system involving a humidification - dehumidification seawater purifier using a concentrator in a parabolic grooved solar air collector. Guarracino et al. [14] presented a dynamic model of PV/T collector with a sheet-and-tube thermal absorber.

Using this model, they estimated yearly electrical energy production and thermal energy gain. Renno [15] developed thermal and electrical model for CPV/T (Concentrated Photovoltaic/Thermal) system and compared with the traditional system in terms of the primary energy and economic saving. Haifei [16] et al. experimentally analyzed high concentrated PV system with dish concentrator. They state that when the concentrator ratio is 200, the electrical efficiency of PV system is about 25%. In their study, Bouadila et al. [17] designed a solar air collector with a latent heat depot system using a spherical capsule and evaluated its performance. In the system they designed, the energy stored in the spheres during the day could be used throughout the night. While the energy efficiency of the experimental system varied between 32% and 45%, the exergy efficiency varied between 13% and 45%.

In the studies conducted so far, different designs were created to increase the performance of solar air collectors. Also, different mathematical models have been developed for the parameters affecting system performance. In contrast to the studies in the literature, in this study, a solar air collector with both a heat storage unit and a concentrator was designed and manufactured. The collector operates according to forced convection conditions and produces the required fan power using the PV modules added to the same system. In this way, in the system, no energy is consumed to heat the air, and the air is heated even when solar radiation is reduced. In addition, as opposed to the other systems, in the system designed with a heat storage unit, a transparent paraffin wax glass and an aluminum panel were used.

In this study, for the first time, the ideal temperatures for heating in winter were increased using the concentrated air collector. Other air collectors cannot reach sufficient temperatures for heating due to low solar radiation during the winter season. Also, the PCMs used in systems cannot be changed practically when their lifetime is over. The microcrystalline PCM collector used in our system was used in the front surface of the collector to ensure interchangeability. Energy analysis was made for the designed and the manufactured system. For the system, the concentrator rate, the heat energy stored in the PCM, and module and collector efficiency were analyzed.

2. Material and Method

In this study, a concentrated solar air collector with a heat depot unit was designed. The design is shown in Fig. 1. The design details of the collector are shown in Fig. 2. The photo of the system produced with these designs is shown in Fig. 3. The system shown in Figs. 1 and 2 includes a Concentrator (1), PV panel (2), a double glass with transparent paraffin wax (3), charge controller (4), solar battery (5), fan (6), fan speed controls (7), and an inverter (8). The energy stored in the batteries using PV panels is used to operate the fan of the air collector. As long as the collector is exposed to the sun, electric energy is stored in the batteries, while heat energy is stored in microcrystalline paraffin wax. Fig. 4 shows the microcrystalline paraffin wax sample. It is between two layers. The layer at the top is made of glass and the one at the bottom is made of aluminum. Sun rays pass through the microcrystalline paraffin wax and heat the aluminum material. Perceptible and latent heat is stored in paraffin through the heated aluminum. During the evening hours when there is no solar radiation, the fan, which is operated by the electrical energy stored in the batteries, transfers the heat energy stored in the paraffin to the environment to be heated.

The designed system is a low concentrator system. In the low concentrator system, concentration rate ranges from 2 to 10. The main advantage of these systems is that they do not need a solar tracking system. Therefore, the initial investment and operating costs of these systems are low.

2.1 Photovoltaic system design

The calculations made for the equipment used in the design are shown below. Equipment capacities and quantities obtained as a result of calculations are shown in Table 1.

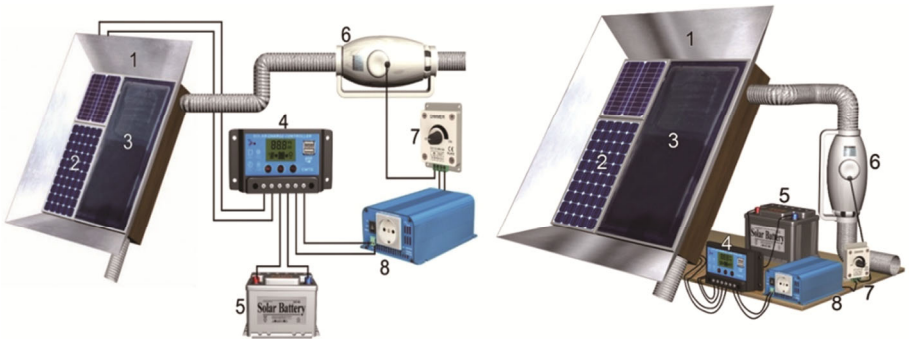

1. Concentrator; 2. Photovoltaic panel; 3. Air collector with heat store; 4. Charge regulator; 5. Solar battery; 6. Fan; 7. Fan speed controllers; 8. Inverter.

Fig. 1 Concentrated photovoltaic panel and solar air collector with a heat depot

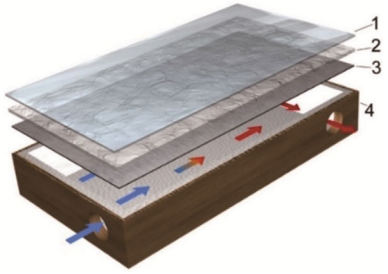

1. Glass; 2. Microcrystalline paraffin wax;
3. Aluminum plate; 4. Collector case.

Fig. 2 Details of the designed air collector with a heat storage unit

Fig. 3 Manufactured concentrated solar air collector with a heat storage unit

Fig. 4 Sample of microcrystalline paraffin wax

Table 1 The equipment properties

Equipment name	Capacity	Quantities
Inverter	100 W	1
Charge regulator	2 A	1
Battery	100 W	1
PV panel	15 W	2
Fan	25 W	1

3. Theoretical Analysis

Microcrystalline paraffin wax was used as the heat storage material in the system. The microcrystalline paraffin wax is completely transparent. Solar radiation can penetrate into it and reach the back side. The thermal specifications of the paraffin used as the heat depot material are shown in Table 2.

The relationship between temperature and enthalpy for the paraffin wax is expressed as follows [18, 19]:

$$h_s = \int_{T}^{T_m} c_s \mathrm{d}T \qquad T \le T_m \qquad \text{solid phase} \tag{1}$$

$$h_l = \int_{T_m}^{T} c_l \mathrm{d}T \qquad T > T_m \qquad \text{liquid phase} \tag{2}$$

Stored heat energy by the paraffin wax can be calculated with Eq. (3) [20]:

$$\dot{Q}_{H_{\text{Total}}} = \dot{Q}_s + \dot{Q}_{lt} + \dot{Q}_l \tag{3}$$

where, $\dot{Q}_s$ is the heat energy in the solid state of paraffin wax; $\dot{Q}_{lt}$ is the heat energy gain during phase change, and $\dot{Q}_l$ is the heat energy in the liquid phase of paraffin wax.

PV panel efficiency includes module efficiency and cell efficiency. Cell efficiency can be calculated with Eq. (4) [21–23]:

$$\eta_c = \eta_0 \left[1 - \beta\left(T_c - 25\right)\right] \tag{4}$$

where η_0 is the standard test efficiency (STC), i.e. ($I_{(t)}$ =1000 W/m^2, T_c = 25°C, AM = 1.5); T_c is the solar cell temperature, and β is thermal coefficient. β value changes according to the structure of the cell. For crystal-silicon, about 0.0045 K^{-1} was taken, while 0.0035 K^{-1}, 0.0025 K^{-1}, and 0.002 K^{-1} were taken for CIS, CdTe, and a-Si, respectively [23]. In this system, polycrystalline silicon PV module was used.

PV panel efficiency can be calculated using Eq. (5):

$$\eta_m = \eta_c \cdot \tau_c \cdot \alpha_c \cdot \delta_c \tag{5}$$

where τ_c is the PV module transparency; α_c is solar cell absorptivity, and δ_c is the packing factor; these parameter values are 0.9, 0.95, and 0.9, respectively [24].

PV module efficiency can also be expressed as in the following equation:

$$\eta_m = \frac{P}{A_m \cdot I_{(t)}} \tag{6}$$

where A_m is the photovoltaic panel area, and P is the power from photovoltaic panels.

Table 2 Microcrystalline paraffin wax thermal specifications [19]

Property	Value
Melting point T_m/°C	47
Density ρ /kg·m^{-3}	818 (Solid), 760 (Liquid)
Latent heat L/kJ·kg^{-3}	266
Thermal conductivity k/W·m^{-1}·K^{-1}	0.24 (Solid and Liquid)
Specific heat c /kJ·kg^{-1}·K^{-1}	2.95 (Solid), 2.51 (Liquid)
Mass/kg	11

The power (P) obtained from the photovoltaic panels can be calculated using Eq. (7).

$$P = V \cdot I \tag{7}$$

The rate of electrical energy gain from the photovoltaic panels was calculated with Eq. (8):

$$\dot{E}_{\mathrm{l}} = \eta_{\mathrm{m}} \cdot A_{\mathrm{m}} \cdot I_{(t)} \tag{8}$$

The overall rate of thermal of the system is expressed in Eq. (9):

$$\dot{Q}_{\mathrm{u,overall}} = \dot{Q}_{H_{\mathrm{Total}}} + \dot{Q}_{\mathrm{SC}} \tag{9}$$

$\dot{Q}_{\mathrm{SC}}$ is the of thermal energy for solar air collector.. This value can be calculated using Eq. (10).

$$\dot{Q}_{\mathrm{SC}} = A \cdot v \cdot \rho \cdot c_p \cdot \Delta T \tag{10}$$

In this equation, v is the average velocity of the air; A, which denotes the cross-section area of air channel, can be calculated as seen below:

$$A = \frac{\pi \cdot D^2}{4} \tag{11}$$

Solar air collector efficiency is obtained using Eq. 12.

$$\eta_{\mathrm{SC}} = \frac{\dot{Q}_{\mathrm{u,overall}}}{I_{(t)} \cdot A_{\mathrm{SC}} + \dot{W}_{\mathrm{f}}} \tag{12}$$

The total efficiency of the experimental setup was calculated as follows:

$$\eta_{\mathrm{Total}} = \eta_{\mathrm{SC}} + \eta_{\mathrm{m}} \tag{13}$$

3.1 Calculation of the concentrator efficiency

In the system, solar radiation was measured from the lower part and the upper part of the concentrator. The concentration ratio (CR) according to the proposed method can be calculated using the Eqs. (14–16) [25, 26]:

$$CR = \frac{I_{t,\mathrm{const}}}{I_{(t)}} \tag{14}$$

where $I_{(t)}$ is the upper part solar radiation, and $I_{t,\mathrm{const}}$ is the lower part or concentrated solar radiation.

The area rate (AR) can be calculated with the rate of the upper concentrator area to the lower concentrator area.

$$AR = \frac{A_{\mathrm{top}}}{A_{\mathrm{panel}}} \tag{15}$$

where A_{top} is upper side area of the concentrator, and A_{panel} is the area of the panel or lower side area of the concentrator. Concentrator efficiency can be written according to the area ratio (AR) and the concentrator rate (CR) as in the following equation:

$$CE = \frac{CR}{AR} \tag{16}$$

3.2 The analysis of uncertainty

The uncertainty analysis is performed to measure the accuracy of the given information. Uncertainties can be calculated using Eqs. (17–20) taking the standard deviations of the measurement device used in the system into account [27, 28]:

$$X_{\mathrm{m}} = \frac{1}{N}\sum_{i=1}^{N} X_i \tag{17}$$

$$S = \left[\frac{1}{(N-1)}\sum_{i=1}^{N}\left(X_i - X_{\mathrm{m}}\right)^2\right]^{1/2} \tag{18}$$

$$a = \frac{1}{\sqrt{N}} \tag{19}$$

$$U = \sqrt{\sum_{i=1}^{R} a_i^2 \cdot S^2} \tag{20}$$

Measurement devices and uncertainty analysis results can be seen in Table 3.

Table 3 Technical characteristics of the equipment used in the experimental system

Devices	Technical properties	Uncertainties
Termo-hygrometer	NTC sensor. Temperature Range: −10°C to +60°C Sensitivity: ±0.5°C Relative humidity measurement range: 0 to 100% RH Sensitivity: ±2.5% RH (0 to 95% RH)	±0.71ºC
Digital solarmeter	Range: 0 to 2000 W/m² Sensitivity: ±5% W/m²	±76.16 W/m²
Anemometer	Range: 0.6 m/s to 20 m/s Sensitivity: ±0.2 m/s	- (Fixed air velocity)

4. Results and Discussions

Solar radiation and duration of sunshine decrease in winter. The decrease in solar radiation leads to a decrease in the temperature of the fluid released from the collector. Due to these low output temperatures in winter, the collectors are not very useful. Although the efficiency of the collectors is high, they are not preferred in winter for their low output temperatures. In order to increase outlet air temperature from the air collectors during the winter season, for the first time a concentrator was used in the system. No studies in the literature have yet focused on concentrated solar air collectors.

In this study, the design and experimental analysis of a concentrated solar air collector with a heat storage unit were carried out for the first time. The solar radiation data obtained from the system are shown in Fig. 5. Concentration rate was calculated as 1.5 using Eq. (14). The designed system with and without a heat storage unit was tested at different times. The initial experiments were performed on the system without the heat storage unit. Fig. 5 shows the concentrated solar radiation values for the system, which was tested with and without

paraffin. The system without the heat storage unit was tested for three days during the winter season. The first graph in Fig. 6 shows the ambient and collector outlet air temperatures of the system without the heat storage unit. It was found that when the outlet air temperature was −10°C, the supply air temperature of the concentrated solar air collector without the heat storage unit reached above 45°C. After the system was filled with micro-crystalline paraffin wax as the heat storage material, it was analyzed experimentally for four days. The solar radiation data for the system with the paraffin wax is shown in Fig. 5.

The thermal energy gain from the collector of the system is shown in Fig. 7. The black graph of Fig. 7 shows the thermal energy gain of the system without the heat storage unit, while the red graph in the figure demonstrates the thermal energy gain of the system with the heat storage unit. In the black graph, the thermal energy gains in the system without the heat storage unit show abrupt fluctuations according to the solar radiation value, but these fluctuations are not observed in the system with the heat storage unit. The thermal energy gains of the system with the heat storage unit are less affected by the sudden changes in solar radiation, and heat can be absorbed for a longer period of time.

Fig. 8 shows the change in sensible and latent heat depot in the paraffin wax over time. The amount of the heat stored increased or decreased parallel to the incoming solar radiation. After 3 p.m., as solar radiation on the collector surface decreased considerably in the winter season, the heat stored in the paraffin began to be used. Therefore, as the graph in Fig. 8 shows, the stored heat decreased. Also, as understood from the graph in Fig. 9 showing the change in system efficiency, efficiency exceeded 100% after 3 p.m. After this time of the day, the energy depot in the paraffin was used without solar radiation input.

Fig. 9 shows the change in collector efficiency over time. Solar collector efficiency is calculated using Eq. (12). In this equation, solar radiation is one of the most important parameters affecting efficiency. As can be seen in the figure, the efficiency of both collectors with and

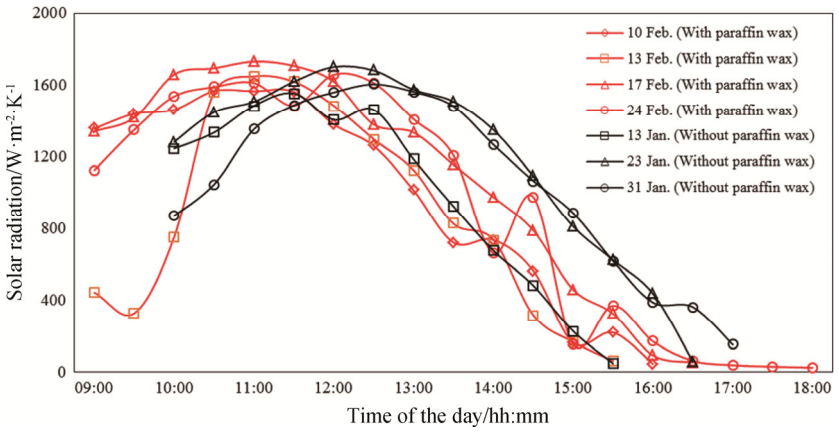

Fig. 5 The variation in concentrated solar radiation

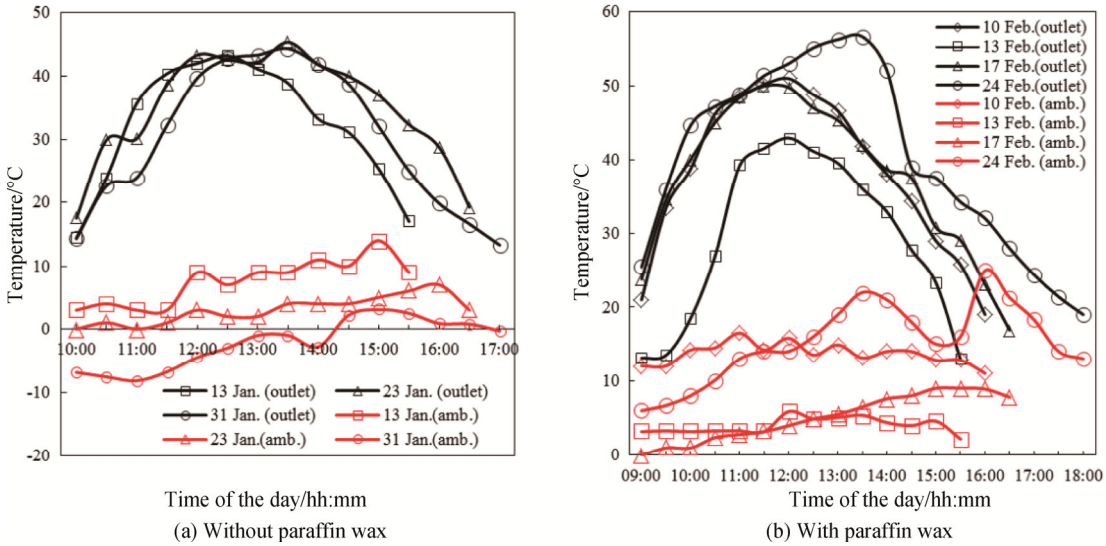

Fig. 6 Solar collector outlet temperature and ambient temperature

without paraffin wax is very close to each other when solar radiation is sufficient during the day. However, with the decrease in solar radiation, a striking difference begins to occur between the collectors. For example, when the change in values obtained from the experiments using paraffin wax on February 24 was examined, it was observed that the collector efficiency started to increase significantly after 4 p.m. This is due to the fact that the paraffin wax continued to transfer heat to the system despite the decrease in solar radiation. For this reason, collector efficiency increased above 100%, especially in areas where solar radiation reduced. While the average collector efficiency of the systems without paraffin wax was 55%, the average collector efficiency of the systems using paraffin wax was calculated as 85%.

The variation in PV module efficiency at different times of certain days is given in Fig. 10. The main reason for these changes is the changes in the ambient

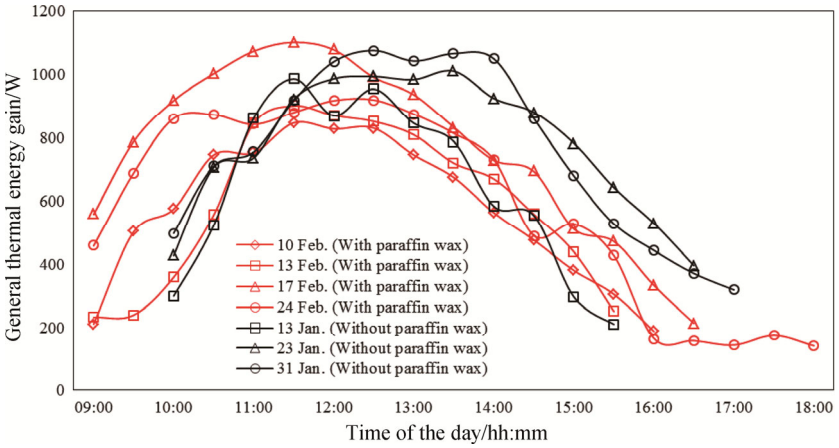

Fig. 7 Thermal energy gains from the system

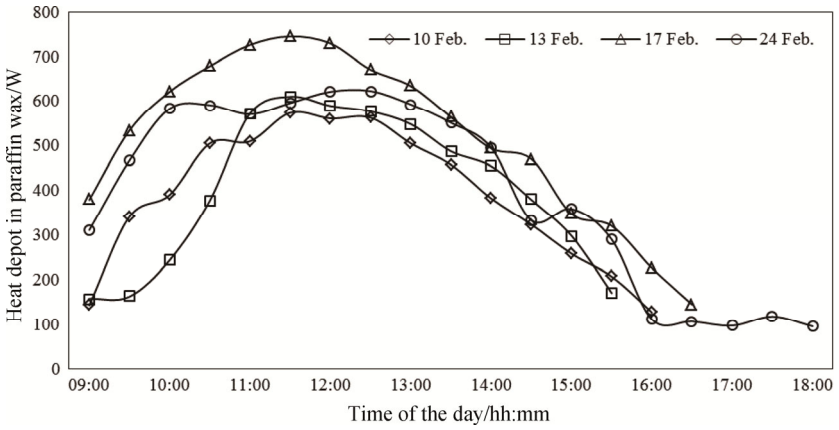

Fig. 8 Heat depot in Paraffin Wax

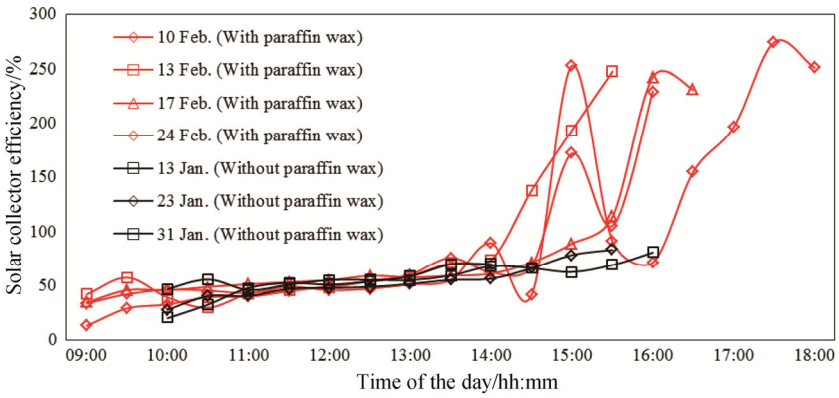

Fig. 9 The variations in solar collector efficiency at different times of the day

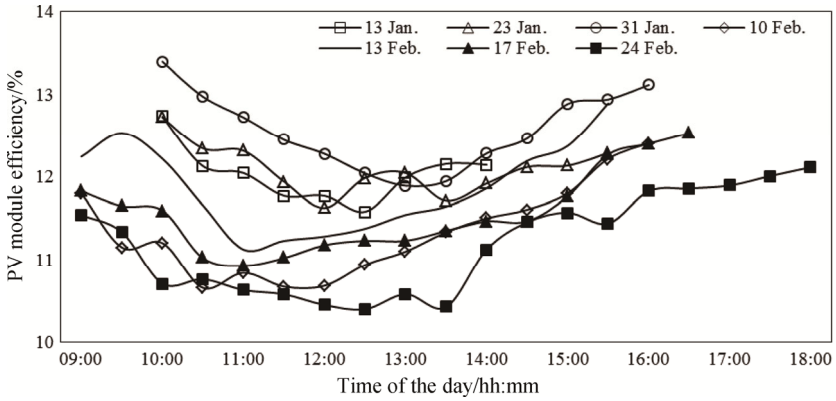

Fig. 10 The variations in PV module efficiency at different times of certain days

temperature on the days of the experiments. For example, during the experiments carried out on January 31, the ambient temperature was at its lowest value (Fig. 6). Thus, the cell temperature decreased, resulting in increased PV module efficiency. While the average PV module efficiency was 13% in the experiments dated January 31, the value was calculated as 11% in the experiments conducted on February 24, when the PV module efficiency was the lowest.

5. Conclusion

The results pertaining to the designed and experimentally analyzed concentrated solar air collector system with a heat storage unit are listed below.

(1) The use of a concentrator in an air collector has made it possible to use the temperature of the air released from the collector. The outlet air temperature from the collector changed between 15°C and 40°C when the outside temperature was about −5°C.

(2) The three-day average efficiency of the concentrated system without the heat storage unit was calculated as 67%.

(3) The average efficiency of the concentrated system with the heat storage unit during the day was calculated as 96%. The system continued to generate heat and electrical energy during the evening hours when there was no solar radiation.

(4) The energy stored in the system with the heat storage unit and the duration of use at night changed depending on the amount of solar radiation during the day.

(5) During the experiments, the duration of use from the system with the heat depot unit in the absence of sun is approximately 4 hours.

(6) Microcrystalline paraffin wax was used as the heat depot. When the paraffin expires, the heat storage process can be continued by easily changing the collector glass.

(7) Although microcrystalline paraffin wax was used for heat storage, normal paraffin wax can also be used. In that case, the surface between glass and aluminum should not be fully filled with paraffin. The solar radiation passing through the other side of the surface, one side of which is filled with paraffin, will heat the black aluminum plate below the paraffin. The aluminum whose temperature increases stores heat by melting the paraffin.

Acknowledgement

Authors thank the Karabük University Scientific Research Projects Coordination Unit for their support for this study. Our project number is KBÜ-BAP-16/ 1-YL-137.

References

[1] Singh S., Dhruw L., Chander S., Experimental investigation of a double pass converging finned wire mesh packed bed solar air heater. Journal of Energy Storage, 2019, 21: 713–723.

[2] Şevik S., Abuşka M., Thermal performance of flexible air duct using a new absorber construction in a solar air collector. Applied Thermal Engineering, 2019, 146: 123–134.

[3] Hu J., Liu K., Guo M., Zhang G., Chu Z., Wang, M., Performance improvement of baffle-type solar air collector based on first chamber narrowing. Renewable Energy, 2019, 135: 701–710.

[4] Zheng W., Zhang H., You S., Fu Y., Zheng, X., Thermal performance analysis of a metal corrugated packing solar air collector in cold regions. Applied Energy, 2017, 203: 938–947.

[5] Abuşka M., Şevik S. Energy, exergy, economic and environmental (4E) analyses of flat-plate and V-groove solar air collectors based on aluminium and copper. Solar Energy, 2017, 158: 259–277.

[6] Gulcimen F., Karakaya H., Durmus, A., Drying of sweet

basil with solar air collectors. Renewable Energy, 2016, 93: 77–86.

[7] Li S., Wang H., Meng X., Wei X., Comparative study on the performance of a new solar air collector with different surface shapes. Applied Thermal Engineering, 2017, 114: 639–644.

[8] El Khadraoui A., Bouadila S., Kooli S., Farhat A., Guizani A., Thermal behavior of indirect solar dryer: Nocturnal usage of solar air collector with PCM. Journal of Cleaner Production, 2017, 148: 37–48.

[9] Bahrehmand D., Ameri M., Gholampour M., Energy and exergy analysis of different solar air collector systems with forced convection. Renewable Energy, 2015, 83: 1119–1130.

[10] Hernández A.L., Quiñonez, J.E., Experimental validation of an analytical model for performance estimation of natural convection solar air heating collectors. Renewable Energy, 2018, 117: 202–216.

[11] Demou A.D., Grigoriadis D.G.E., 1D model for the energy yield calculation of natural convection solar air collectors. Renewable Energy, 2018, 119: 649–661.

[12] Al-damook A., Khalil W.H., Experimental evaluation of an unglazed solar air collector for building space heating in Iraq. Renewable Energy, 2017, 112: 498–509.

[13] Al-Sulaiman F. A., Zubair, M. I., Atif, M., Gandhidasan, P., Al-Dini, S. A., & Antar, M. A., Humidification dehumidification desalination system using parabolic trough solar air collector. Applied Thermal Engineering, 2015, 75, 809–816.

[14] Guarracino I., Mellor A., Ekins-Daukes N.J., Markides, C.N., Dynamic coupled thermal-and-electrical modelling of sheet-and-tube hybrid photovoltaic/thermal (PVT) collectors. Applied Thermal Engineering, 2016, 101: 778–795.

[15] Renno C., Thermal and electrical modelling of a CPV/T system varying its configuration. Journal of Thermal Science, 2019, 28(1): 123–132.

[16] Chen H., Li G., Yang J., Zhang F., Liang M., Ji J., Experimental and Comparison Study on Two Solar Dish Systems with a High Concentration Ratio. Journal of Thermal Science, 2019, 28(6): 1205–1211.

[17] Bouadila S., Kooli S., Lazaar M., Skouri S., Farhat A., Performance of a new solar air heater with packed-bed latent storage energy for nocturnal use. Applied Energy, 2013, 110: 267–275.

[18] Ceylan İ., Gürel A.E., Ergün A., Tabak A. Performance analysis of a concentrated photovoltaic and thermal system. Solar Energy, 2016, 129: 217–223.

[19] Lee J.S., Lucyszyn S., Thermal analysis for bulk-micromachined electrothermal hydraulic microactuators using a phase change material. Sensors and Actuators A: Physical, 2007, 135(2): 731–739.

[20] Mishra R.K., Tiwari G.N., Energy and exergy analysis of hybrid photovoltaic thermal water collector for constant collection temperature mode. Solar Energy, 2013, 90: 58–67.

[21] Zondag H.A., Flat-plate PV-Thermal collectors and systems: A review. Renewable and Sustainable Energy Reviews, 2008, 12(4): 891–959.

[22] Ramos A., Chatzopoulou M.A., Guarracino I., Freeman J., Markides C.N., Hybrid photovoltaic-thermal solar systems for combined heating, cooling and power provision in the urban environment. Energy Conversion and Management, 2017, 150: 838–850.

[23] Acar B., Gürel A.E., Ergün A., Ceylan I., Ağbulut Ü., Can A., Performance assessment of a novel design concentrated photovoltaic system coupled with self-cleaning and cooling processes. Environmental Progress & Sustainable Energy, 2020. DOI: 10.1002/ep.13416.

[24] Machniewicz A., Knera D., Heim D., Effect of transition temperature on efficiency of PV/PCM panels. Energy Procedia, 2015, 78: 1684–1689.

[25] Ceylan İ., Gürel A.E., Ergün A., The mathematical modeling of concentrated photovoltaic module temperature. International Journal of Hydrogen Energy, 2017, 42(31): 19641–19653.

[26] Ustaoglu A., Alptekin M., Okajima J., Maruyama S., Evaluation of uniformity of solar illumination on the receiver of compound parabolic concentrator (CPC). Solar Energy, 2016, 132: 150–164.

[27] Ceylan İ., Gürel, A.E., Solar-assisted fluidized bed dryer integrated with a heat pump for mint leaves. Applied Thermal Engineering, 2016, 106: 899–905.

[28] Ceylan İ., Kaya M., Gürel A.E., Ergun A., Energy analysis of a new design of a photovoltaic cell-assisted solar dryer. Drying Technology, 2013, 31(9): 1077–1082.